SCIENTIFIC REPORTS

OPEN

SUBJECT AREAS:
EXPERIMENTAL MODELS OF DISEASE
ION TRANSPORT
BREAST CANCER
MECHANISMS OF DISEASE

Received
10 September 2014

Accepted
23 December 2014

Published
10 February 2015

Correspondence and requests for materials should be addressed to W.S. (W.Schreibmayer@gmx.at)

* Current address: Department of Dentistry, Medical University of Graz, Harrachgasse 21/4 A-8010 Graz, Austria.

Piezo1 forms mechanosensitive ion channels in the human MCF-7 breast cancer cell line

Chouyang Li[1], Simin Rezania[1], Sarah Kammerer[1], Armin Sokolowski[1]*, Trevor Devaney[1], Astrid Gorischek[1], Stephan Jahn[2], Hubert Hackl[3], Klaus Groschner[1], Christian Windpassinger[4], Ernst Malle[5], Thomas Bauernhofer[6] & Wolfgang Schreibmayer[1]

[1]Department of Biophysics, Medical University of Graz, Graz, Austria, [2]Department of Pathology, Medical University of Graz, Graz, Austria, [3]Division of Bioinformatics, Biocenter, Innsbruck Medical University, Innsbruck, Austria, [4]Department of Human Genetics, Medical University of Graz, Graz, Austria, [5]Institute of Molecular Biology and Biochemistry, Medical University of Graz, Graz, Austria, [6]Division of Oncology, Department of Internal Medicine, Medical University of Graz, Graz, Austria.

Mechanical interaction between cells – specifically distortion of tensional homeostasis-emerged as an important aspect of breast cancer genesis and progression. We investigated the biophysical characteristics of mechanosensitive ion channels (MSCs) in the malignant MCF-7 breast cancer cell line. MSCs turned out to be the most abundant ion channel species and could be activated by negative pressure at the outer side of the cell membrane in a saturable manner. Assessing single channel conductance (G_A) for different monovalent cations revealed an increase in the succession: $Li^+ < Na^+ < K^+ \approx Rb^+ \approx Cs^+$. Divalent cations permeated also with the order: $Ca^{2+} < Ba^{2+}$. Comparison of biophysical properties enabled us to identify MSCs in MCF-7 as ion channels formed by the Piezo1 protein. Using patch clamp technique no functional MSCs were observed in the benign MCF-10A mammary epithelial cell line. Blocking of MSCs by GsMTx-4 resulted in decreased motility of MCF-7, but not of MCF-10A cells, underscoring a possible role of Piezo1 in invasion and metastatic propagation. The role of Piezo1 in biology and progression of breast cancer is further substantiated by markedly reduced overall survival in patients with increased Piezo1 mRNA levels in the primary tumor.

The single cell, as elementary building block of an organ, steadily encounters physical forces such as hydrostatic pressure, shear, compression and tension. Via force-dependent activation of signaling cascades, cells dynamically adapt and respond to mechanical cues by modifying their behavior and remodeling of the microenvironment[1–3]. Together with hormonal and growth cues, force shapes cellular architecture of the mammary gland at all stages of development and function[4–6]. The balance between forces and cellular reactions is pivotal to maintain adult tissue homeostasis and, as a consequence, distortion or loss of this equilibrium leads to pathology, including cancer[7,8]. Several molecular entities that perceive and integrate forces (*mechanoreceptors*) have evolved in mammalian cells, amongst them various transmembrane ion channel proteins[9,10]. The transient receptor potential (Trp) ion channel family is represented by dozens of genes within the human genome and their members are generally activated by environmental stimuli such as temperature, pH, osmolarity, pheromones and taste compounds[11]. In addition, ion channels formed by particular Trp subunits have also been identified to act as mechanosensitive ion channels (MSCs)[11,12]. Other promising candidates for mechanotransduction in mammals comprise TMC and Piezo proteins, which represent two recently discovered mechanically gated ion channel families[13,14]. The role of ion channels as molecular actors contributing to virtually all hallmarks of cancer cells is still emerging[15]. Given the importance of mechanosensation for development and tissue homeostasis of normal mammary gland, its role in cancerogenesis and subsequent metastasation, we have studied MSCs within the plasma membrane of the malignant human MCF-7 breast cancer cell line. Permeation properties of ion channel proteins, i.e. single channel conductance and selectivity for certain kinds of ions, represent highly specific features that can be used to identify peculiar types of ion channels and even to distinguish between orthologs of subtypes from different species (see e.g.: http://www.guidetopharmacology.org/). In order to identify the molecular architecture of MSCs in MCF-7 cells, we characterized and compared this biophysical fingerprint to the recently discovered MSC protein Piezo1. In order to investigate the contribution of Trp ion channel subunits, we have

engineered a cell line, based on MCF-7 wild type (MCF-7^{WT}) that permanently overexpresses a dominant negative TrpC subunit (MCF-$7^{TrpC\_k.o}$) und studied whether the density of MSCs is affected by knockout of functional TrpC channels. The benign human MCF-10A mammary epithelial cell (MEC) line was studied in order to investigate whether the existence of MSCs is a peculiar feature of malign MECs. As Ca^{2+} permeable MSCs have been shown to play an important role in cell motility and migration[16], we investigated whether block by the tarantula toxin GsMTx-4 influenced motility of the two MEC lines studied. Finally we have analyzed whether expression levels for the mRNA encoding the MSC of MCF-7 cells in primary tumors has an influence on prognosis for patients suffering from breast cancer.

Methods

Solutions (mmole/L): Zeroing Bathing Solution (ZBS). K^+/Asp^-(120), KCl (20), $MgCl_2$ (4), NaCl (10), $EGTA^-$/K^+ (10), $HEPES^-$ (10), buffered with K^+ to pH:7.4. *Pipette Filling Solution (PFS):* KCl (153), $MgCl_2$ (4), $CaCl_2$ (1), $GdCl_3$ (0.2), $HEPES^-$ (10) buffered with K^+ to pH:7.4. *PFS/Li^+ (PFS/Na^+; PFS/Rb^+; PFS/Cs^+; PFS/(K^+:Na^+)):* as PFS, but K^+ was replaced by the appropriate cation or a mixture of K^+ and Na^+ at a 1 : 1 ratio. *PFS/Ca^{2+} (PFS/Ba^{2+}):* $CaCl_2$ (or $BaCl_2$; 100), $MgCl_2$ (4), $CaCl_2$ (1), $GdCl_3$ (0.02), $HEPES^-$ (10) buffered with K^+ to pH:7.4. Lyophilized GsMTx-4 was obtained from Alomone Labs (Cat.#: STG-100, Jerusalem, Israel) and reconstituted at a concentration of 90 μmole/L. Aliquots were shock frozen in liquid N_2 and stored at −30°C until use. All reagents used were of reagent grade unless stated otherwise.

Cell culture. MCF-7, MCF-10A and HEK-293 cells were cultured as described[17,18]. Medium was changed every 2–3 days. Confluent cells were detached split 1 : 10 and transferred to fresh culture flasks.

Molecular Biology. RNA isolation and cDNA synthesis was performed as described[17]. Six ng cDNA were subjected to PCR for gene quantification (QuantiFast SYBER Green PCR kit, Qiagen GmbH) using Light Cycler 480 system (40 Cycles; Roche Diagnostics). The following primers (designed with Primer3 (http://primer3.ut.ee/.)) were used: Piezo1 (NCBI Reference Sequence, NM_001142864.2): forward: 5′-CATCTTGGTGGTCTCCTCTGTCT-3′; reverse: 5′-CTGGCATCCACATC-CCTCTCATC-3′. GAPDH: forward: 5′-ATGGGGAAGGTGAAGGTCG-3′; reverse: 5′-GGGGTCATTCATGGCAACAATA-3′. Relative mRNA expression levels of Piezo1 gene compared to the housekeeping gene (GAPDH) were calculated using $2^{-\Delta\Delta C_T}$ method[19]. HEK-293 cells were transfected with the biscistronic pIRES2 plasmid containing human Piezo1 and an enhanced variant of the green fluorescence protein (eGFP) using the Transfast™ reagent (Promega) and MCF-10A cells with Lipofectamine™ 2000 (InVitrogen) according to the manufacturers' suggestions. Transfected HEK-293 cells were used within 24 to 48 h and MCF-10A within 24 h after transfection. The MCF-$7^{TrpC\_k.o.}$ cell line, stably expressing a dominant negative TrpC construct[20], was generated by adding Geneticin (G418; an aminoglycoside antibiotic that blocks translation; LifeTech Company; Order No.: 11811-031; 3 mg/mL) 72 h after Transfast™ transfection. Successful expression was monitored by fluorescence of the chimeric k.o subunit that was fused to a yellow variant of the green fluorescence protein (eYFP). The cells were kept in culture for 14 days, prior to selecting stable clones. G418 was removed 48 h before experimentation was started.

Electrophysiology. Cells were seeded on coverslips 24 to 72 h before electrophysiological experiments were started (Coverslips for HEK-293 cells were coated with polylysine) and kept in the incubator. No longer than 20 minutes before actual recording was started, coverslips were transferred to a custom-made bathing chamber that was mounted to the stage of an inverted microscope (IM35, Zeiss, Germany). Cells were washed and superfused with *ZBS*. Patch clamp pipettes were pulled from borosilicate glass capillaries (outer diameter: 1.6 mm, inner diameter: 1.0 mm; final resistance was 1–2.5 MΩ), coated with Sylgard (Sylgard 184, Dow Corning), fire-polished with a custom-made micro forge and filled with the appropriate PFS. After successful establishment of a Gigaseal, single channel currents were recorded at constant potential using an Axopatch-200B or Axopatch-1D amplifier (Molecular Devices, USA). Single MSC channels were activated by applying negative pressure to the interior of the patch clamp pipette (0–200 mbar). Negative pressure was exerted via a 1 mL disposable syringe that was attached to the pipette holder and also used for establishing the Gigaseal. The amount of negative pressure in the pipettes interior was measured via a semiconductor based pressure sensor implemented into a self-built electronic device (ASDXRRX005PDAA5; Honeywell, Golden Valley, MN, U.S.A.). Current traces were low pass filtered at 2 kHz and digitized at 20 kHz using the Digidata 1322A interface (Molecular Devices, USA) using the Clampex 9.2 software (Molecular Devices, USA). Traces were digitally low pass filtered at 1500 Hz and analyzed using the Clampfit 10.3 software (Molecular Devices, USA). Single channel conductances (G_Λ) were assessed by linear regression of current amplitudes in the range V_p: *-40 mV* to V_p: *-140 mV* (both in the outward and the inward direction). The activation of single MSC channels was assessed by fitting the average current flowing through the open channels at a given time interval ($\hat{I}.t^{-1}$ (pA.ms^{-1}; nC)), normalized to the maximum (f_a; fractional activation), as a function of negative pressure (*n.p.* (mbar)) at the extracellular side, to equation (1):

$$f_a = \frac{1}{1 + e^{-\frac{n.p. - EP_{50}}{b}}} \quad (1)$$

Where EP_{50} represents the n.p. required for half maximal activation of MSCs and b the slope of the sigmoidal function at EP_{50}. In our initial observations of MSCs in the MCF-7^{WT} cell line, *PFS* without addition of Gd^{3+} ions was used in the patch clamp pipette. Addition of Gd^{3+} at 20 μmole/L, a concentration known to block most MSCs based on subunits of the Trp channel family[21], did not produce detectable effects on MSCs in MCF-7 cells (supplementary Figure 1) and was used subsequently.

Cell observer and motility. Cells were split and seeded to 24 well plates at densities of *1*10^4 cells/well* (MCF-7) and *2.5*10^3 cells/well* (MCF-10A), approx. 24 h before observation by the cell observer (Axiovert200M, Zeiss, Germany). GsMTx-4 was added to the appropriate wells immediately before frame acquisition was started. Frames were acquired every 20 minutes for a total time interval of 72 h. Individual cells were tracked using the ImageJ software (v1.47; Wayne Rasband, NIH, http://imageJ.NIH.gov/) using the manual tracking plugin. Cell coordinates were recorded and analyzed using Microsoft Excel 2010 and routines written in Visual Basic for Applications (version 7.0). The 2D motility coefficient (MC (μm^2.min^{-1})) was calculated from the slope ($D^2/\Delta t$) of the linear regression of the squared distance (D^2) as a function of time interval Δt (Δt_{max}=10 h) according to equation (2) as described[22]:

$$MC = \frac{D^2}{4.\Delta t} \quad (2)$$

Statistical analysis and bioinformatics. Statistical analysis was performed using SigmaPlot/SigmaStat (version 12.5, Systat Software, USA). Experimental parameters were first tested for normal distribution. Subsequently, tests for statistical significance were performed (One Way ANOVA or Kruskal-Wallis test), followed by the appropriate pairwise multiple comparison procedures. The overall survival curves based on Piezo1 (Fam38A; affymetrix ID: 202771_at) mRNA expression was calculated by the "KMPlotter" tool using the "autoselect best cutoff" function (http://kmplot.com/analysis/;[23]) using the breast cancer database (version 2014; N=1115).

Results

Upon application of mechanical stress, functional MSCs were detected in 54% of cell attached membrane patches derived from MCF-7 cells (Figure 1A, Table 1). The next frequently observed ion channel within the plasma membrane of MCF-7 cells was a constitutively active, highly K^+ selective, inward rectifying ion channel with an inward single channel conductance of approx. 70pS in PFS (supplementary Figure 2). Since this ion channel, in comparison to MSCs, was observed in only 9 out of 96 patches in MCF-7^{WT} cells (≈9%) and other species of ion channels were observed only once, we conclude that MSCs represent a major ion channel population of the malignant MCF-7 breast cancer cell line. MSC activity depended on the strength of negative pressure (n.p.) applied in a saturable manner. Half maximal n.p. for activation (EP_{50}; Figure 1b, Table 2) in MCF-7 cells was similar to EP_{50} values observed for Piezo1, a recently discovered MSC subunit, overexpressed in HEK-293 cells[13,24]. Single MSC conductance (G_Λ) was measured for cation flux across the plasma membrane from the extracellular compartment inside the cytosol and in the opposite direction. At the same absolute value of pipette potential (V_p) applied, I_Λ was greater in the inward than in the outward direction (Figure 2). The G_Λ observed for inward currents carried predominantly by K^+ ions was 25.6 pS (Table 3). This value is close to that reported for murine Piezo1 (mPiezo1) overexpressed in HEK-293 cells[13]. Although both EP_{50} and G_Λ values, respectively, are indicative that Piezo1 protein may be the component of MSCs in MCF-7 cells, members of other ion channel families have also be considered as possible candidates for MSCs formation in mammalian cells[10]. Moreover, G_Λ of mPiezo1 has been reported to be variable, since it is blocked by divalent cations, such as Mg^{2+}, Ca^{2+} and Zn^{2+} and hence the close similarity in G_Λ's observed may be misleading[25]. In order to gather additional biophysical distinguishing marks that may allow the identification of the molecular nature of MSCs in MCF-7 cells we assessed G_Λ for different monovalent and divalent cations under standardized conditions (Figure 3). G_Λ was

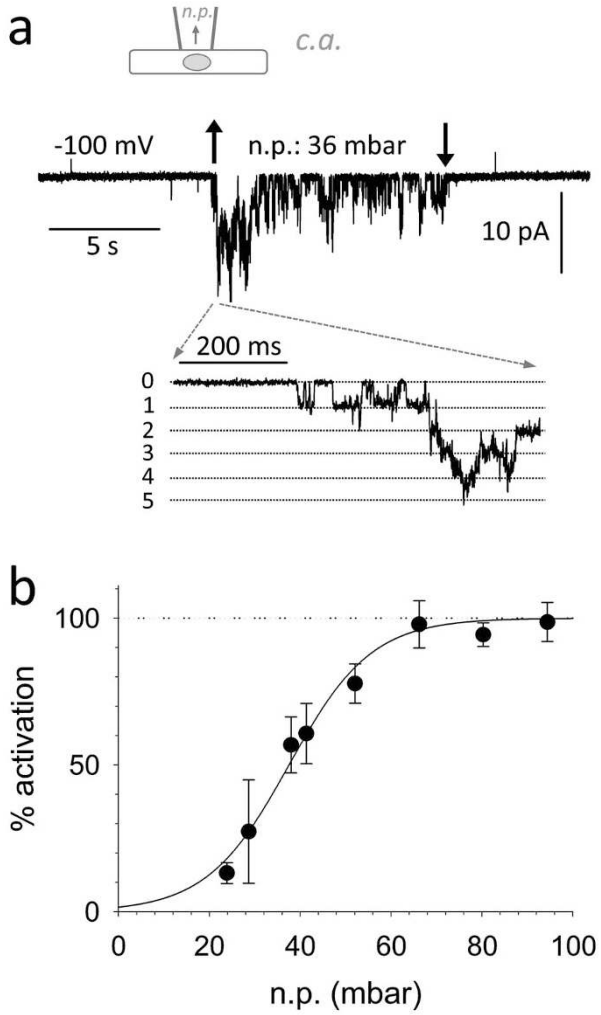

Figure 1 | Mechanosensitive ion channels in the MCF-7 cell line. (1a).: Original registration derived in the cell attached configuration (shown schematically at top). Mechanical stress was induced by applying negative pressure (n.p.) inside the pipette (indicated by arrows). (1b).: Open probability (in % of maximum activation) as a function of negative pressure applied (N=18).

significantly reduced when Li^+ or Na^+ were used as permeant monovalent cations with the succession $Li^+ < Na^+ < K^+ \sim Rb^+ \sim Cs^+$. Also divalent cations permeated considerably, but at significantly reduced G_Λ's, when compared to K^+ under the experimental conditions used. G_Λ was also significantly smaller for Ca^{2+} compared to Ba^{2+} (see Figure 3c for G_Λ's for different cations). In summary, both distinct and significant differences in G_Λ, the rate of ion permeation across an open MSC, were observed. Ion selectivity of MSCs (measured by the quotient of permeability coefficients (P_{X^+}/P_{K^+}) of the respective ion

Table 1 | Frequency of occurrence of MSCs in the cell lines used

	Total number of patches	Number of patches with MSCs	% of patches with MSCs
MCF-7^{WT}	291	157	54%
MCF-7$^{TrpC_k.o*}$	39	22	56%
HEK-293^{WT}	16	0	0%
HEK-293^{hP1}	60	44	73%
MCF-10A^{WT}	30	0	0%
MCF-10A^{hP1}	45	28	62%

*: stably expressing cell line.

Table 2 | Activation of MSCs by negative pressure in the different breast cancer cell lines studied

	EP_{50} ± SEM (mm Hg)	b ± SEM(mm Hg^{-1})	N
MCF-7^{WT}	40.8 ± 1.1	9.1 ± 1.0	18
MCF-10A^{hP1}	38.7 ± 1.1	5.9 ± 1.1	4

(P_{X^+}), normalized to the permeability coefficient for K^+ (P_{K^+})), was calculated from the observed reversal potential of single channel currents (I_Λ's; supplementary Table 1). The ratio $P_{Ca^{2+}}/P_{K^+}$ (0.40

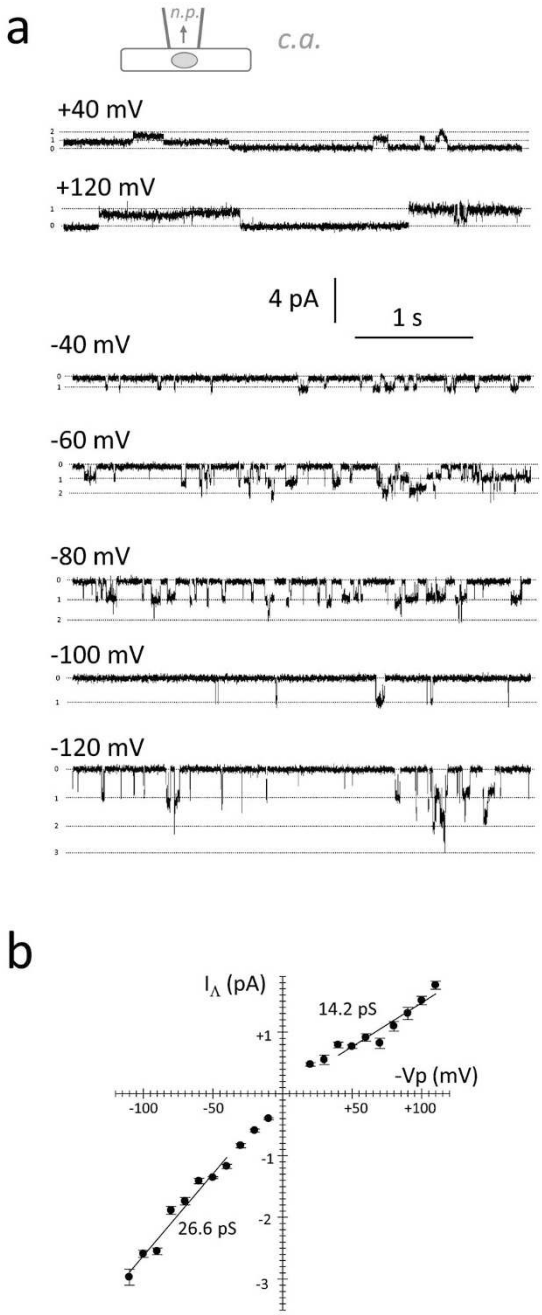

Figure 2 | Single channel conductance properties of MSC in the MCF-7 cell line. (2a).: Original registrations recorded at different potentials during mechanical stress (configuration shown schematically at top). K^+ ions (153 mmole/L) were carrying the inward single channel currents at negative potentials. (2b).: I/V relation for the single channel currents shown in (2a).

Table 3 | Single channel properties of MSCs in the MCF-7^{WT} cell line (*PFS*)

	Mean ± SEM	N
E_{rev} *(mV)*	7.3 ± 1.2	8
G_Λ *(pS); inward*	25.6 ± 0.4	8
G_Λ *(pS); outward*	20.6 ± 2.1	8

± 0.04; N=4) was significantly lower for Ca^{2+} when compared to K^+, but Ca^{2+} permeation was still substantially as indicated by G_Λ. Ion permeability ratios were close to 1 for the other cations tested (Supplementary Figure 2). The specific differences in G_Λ's observed for different cations led us to overexpress hPiezo1 in HEK-293 cells and to characterize the resulting MSCs. q-PCR analysis revealed that mRNA encoding Piezo1 was overexpressed >100 fold in transiently transfected cells, when compared to HEK-293^{WT} (Figure 4e). Accordingly, MSCs that were not observed in HEK-293^{WT} cells were frequently recorded from transfected HEK-293^{hP1} ones (Figure 4a&b; Table 1). Next, G_Λ 's of the resulting MSCs at chosen ion compositions were characterized (Figure 4c&d). Single channel conductance was significantly smaller ($p<0.001$) when Li^+ was used as charge carrier. Ca^{2+} alike MSCs recorded from MCF-7^{WT}, permeated also. G_Λ's assessed for Li^+, K^+, Ca^{2+} and Na^+:K^+ (at a molar ratio of 1 : 1) were indistinguishable from those of MSCs recorded from MCF-7 cells (Figure 4d). The peculiar G_Λ's for different cations observed by us strongly suggest that MSCs in MCF-7 are composed of Piezo1 protein. In order to generate additional data that would allow MSC identification, we have engineered a MCF-7 based cell line overexpressing a dominant negative TrpC subunit (MCF-7$^{TrpC_k.o}$). Overexpression of the ion permeation deficient subunit is expected to eliminate currents through channels formed by TrpC proteins that are known homo- or heteromerization partners of TrpC1, TrpC3, TrpC4, TrpC6 and TrpC7[20]. Provided involvement of TrpC subunits in MSC formation, a significant reduction in the number of functional ion channels is expected in the MCF-7$^{TrpC_k.o}$ cell line. After all, the frequency of occurrence of functional MSCs in both cell lines was similar, suggesting that TrpC subunits are not involved (Table 1).

MCF-7 cells have been cultivated from invasive ductal carcinoma and exert the luminal gene cluster subtype signature[26]. Subsequently we investigated whether non-cancerous breast cells do also possess functional MSCs at the surface. Accordingly, the MCF-10A line, derived from human fibrocystic mammary tissue and representing an immortal non neoplastic MEC line[27] was used as a model for normal mammary gland cells. Under the experimental conditions used we could not detect functional MSCs in MCF-10A cells (Figure 5a; Table 1). In addition, q-PCR revealed that mRNA encoding Piezo1 is substantially reduced in MCF-10A compared to MCF-7 cells, but not entirely absent (Figure 5d, right). When cDNA encoding human Piezo1 was overexpressed transiently in MCF-10A cells, endogenous Piezo1 mRNA levels increased >10 fold (Figure 5D, left). Consequently MSCs with single channel conductance indistinguishable from those obtained from HEK-293 cells were observed (Figure 5c; supplementary Figure 3). The results indicate that MCF-10A cells are able to express MSCs formed by Piezo1 protein, but endogenous expression is not sufficient to form functional channels.

Migration, motility and invasion represent essential hallmarks of cancer cells, important for malignancy and metastasation[28].

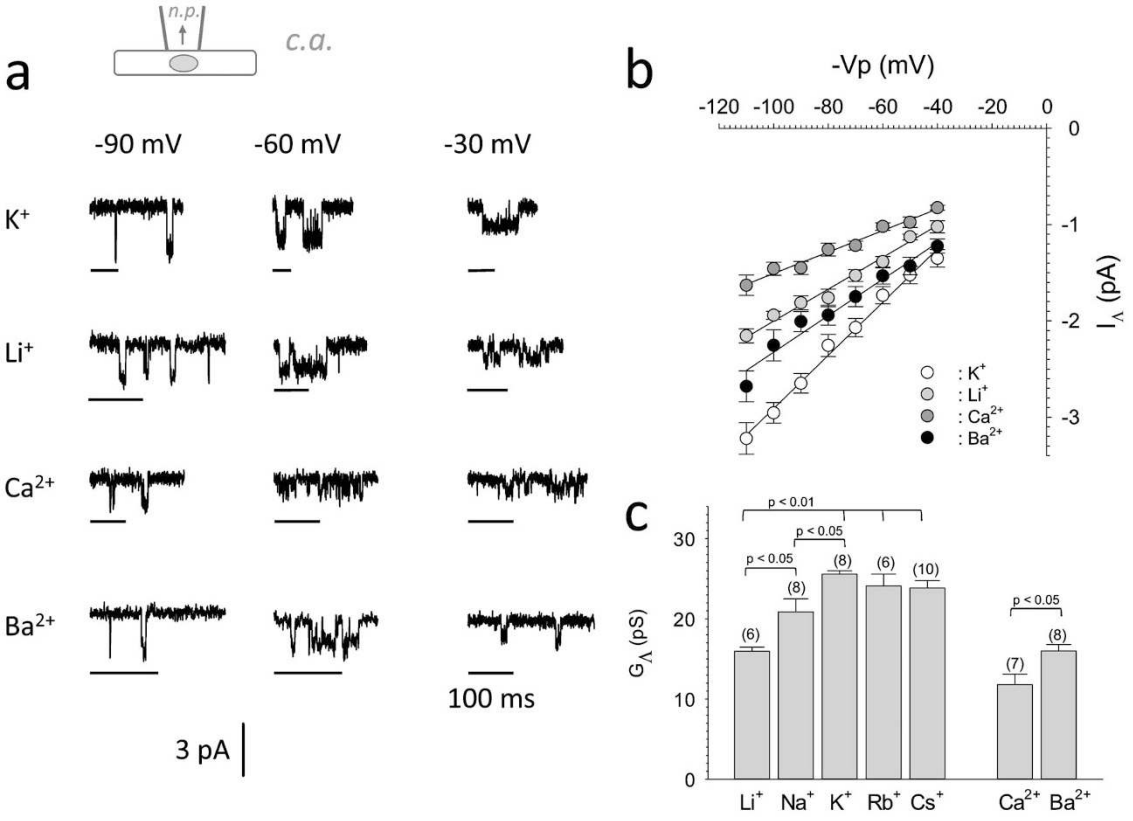

Figure 3 | Ion selectivity profile of MSC in MCF-7 cell line. (3a).: Original registrations of single channel inward currents recorded in the cell attached configuration at three different potentials during mechanical stress. Different ions were used as charge carriers for the inward currents (153 mmole/L were used in case of monovalent cations and 100 mmole/L in case of divalent cations). (3b).: Average I/V relations for single I_Λ inward currents carried by different cations (N= 6–10). Symbols denote mean values ± SEM, line denotes linear regression through the data. (3c).: Ion selectivity profile of inward single channel conductance carried by different mono- and divalent cations. Number of individual experiments is shown at the top of each bar in parenthesis. Mean values ± SEM are shown.

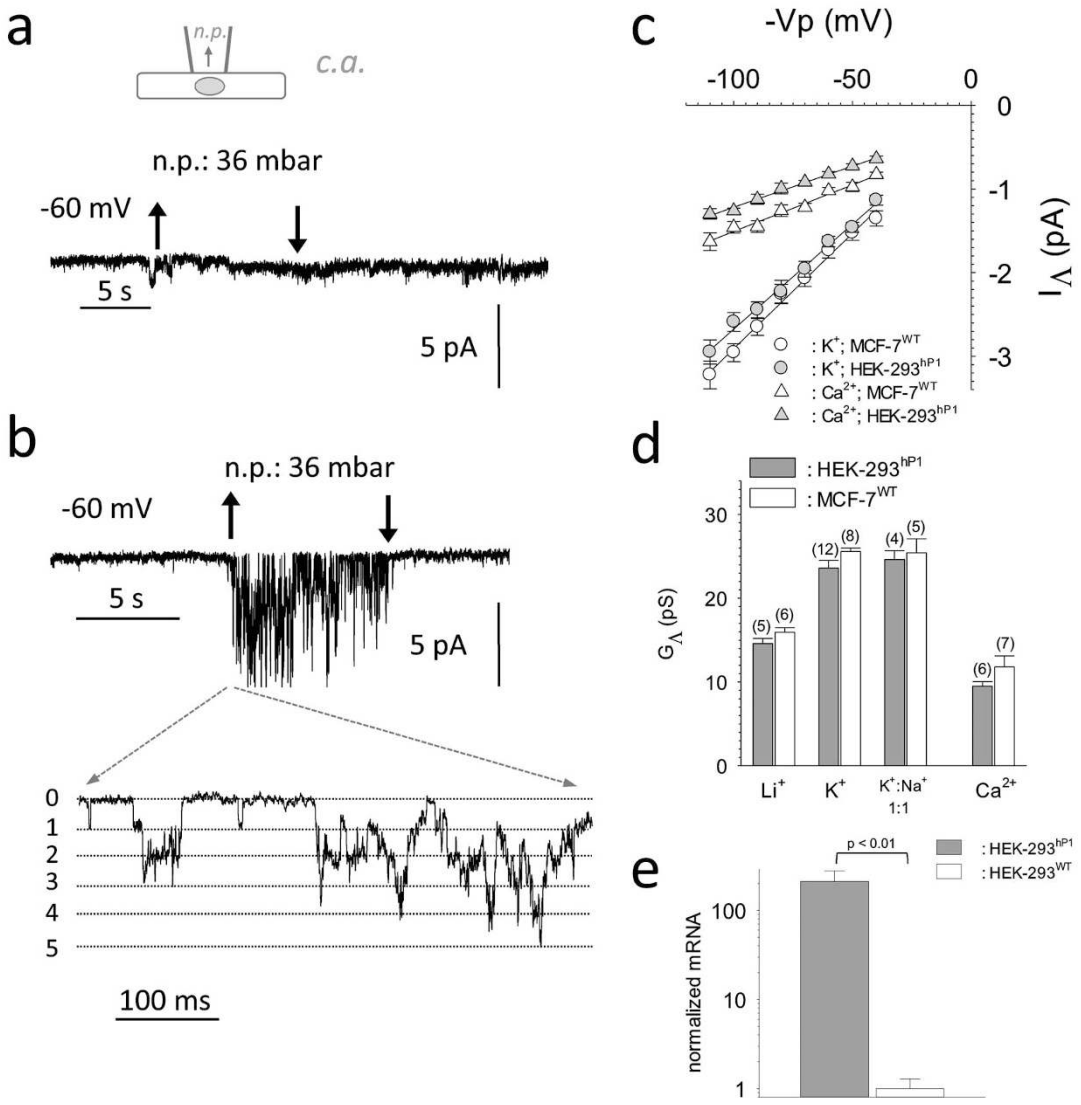

Figure 4 | Single channel conductance properties of hPiezo1 expressed in the HEK cell line. (4a).: Original registration from untransfected HEK-293 cell (configuration shown schematically at top). (4b).: same as 4a, but cell was transfected with biscistronic pIRES2 containing hPiezo1 and eGFP as inserts. (4c).: Average I/V relations for single I_Λ inward currents carried by 153 mmole/L K^+ (grey circles) and 100 mmole/L Ca^{2+} (grey triangles). White symbols denote I_Λ's recorded from MCF-7 cells, lines represent a linear regression through the data (N = 5–8). (4d).: Ion selectivity profile of inward single channel conductance carried by different mono- and divalent cations and by Na^+:K^+ at a 1:1 ratio. Number of individual experiments is shown at the top of each bar in parenthesis. Mean values ± SEM is shown. (4e).: Quantitative RT-PCR assessing the fold increase in the number of hPiezo1 mRNA transcripts upon transient transfection of HEK-293 cells with the pIRES2 construct (data were derived from 3 individual transfection experiments). Mean values ± SEM are shown.

Moreover, Ca^{2+} permeable MSCs have been shown to be pivotal for cell motility and migration[16]. Subsequently we investigated whether MSCs formed by Piezo1 may regulate these cellular properties. Motility and velocity of MCF-7^{WT} cells were studied in the absence and in the presence of GsMTx-4 (Figure 6a&b), a peptide toxin from Chilean rose tarantula venom, known to block functional Piezo1 channels[29]. Both cellular velocity and motility of MCF-7^{WT} cells were reduced by the presence of GsMTx-4 (Figure 6c&d). In contrast to MCF-7, GsMTx-4 did not affect velocity or motility of MCF-$10A^{WT}$ cells (supplementary Figure 4). This finding further supports a role of Piezo1 in motility of the cancerous MCF-7 cell line. The observations derived from models of benign and malign MECs prompted us to investigate whether overexpression of mRNA encoding Piezo1 in the primary tumor may be related to clinical outcome in breast cancer patients. A dataset generated from GEO and comprising overall survival data for 1115 patients was used (dataset version 2014)[23]. Overall survival times of breast cancer patients with low mRNA expression for Piezo1 in the primary tumor turned out to be significantly longer when compared to patients with high expression levels (Figure 7). This finding is of strong support that high levels of Piezo1 in the tumor have causal and profound impact on disease progression.

Discussion

Here we report for the first time the existence of functional mechanosensitive ion channels in a malignant human MEC line. Single channel analysis revealed that Ca^{2+} permeation of MSCs in the MCF-7 line is substantial. Furthermore, characteristic differences in G_Λ for Li^+ and Na^+, the smallest alkali metal ions tested, were found when compared to G_Λ for other alkali metal ions (K^+, Rb^+, Cs^+). Among monovalent and divalent cations studied, G_Λ was inversely related to the radius of the hydrated ion suggesting that these ions may pass the open pore in the hydrated configuration. Several facts prompted us to identify Piezo1 as a component of MSCs

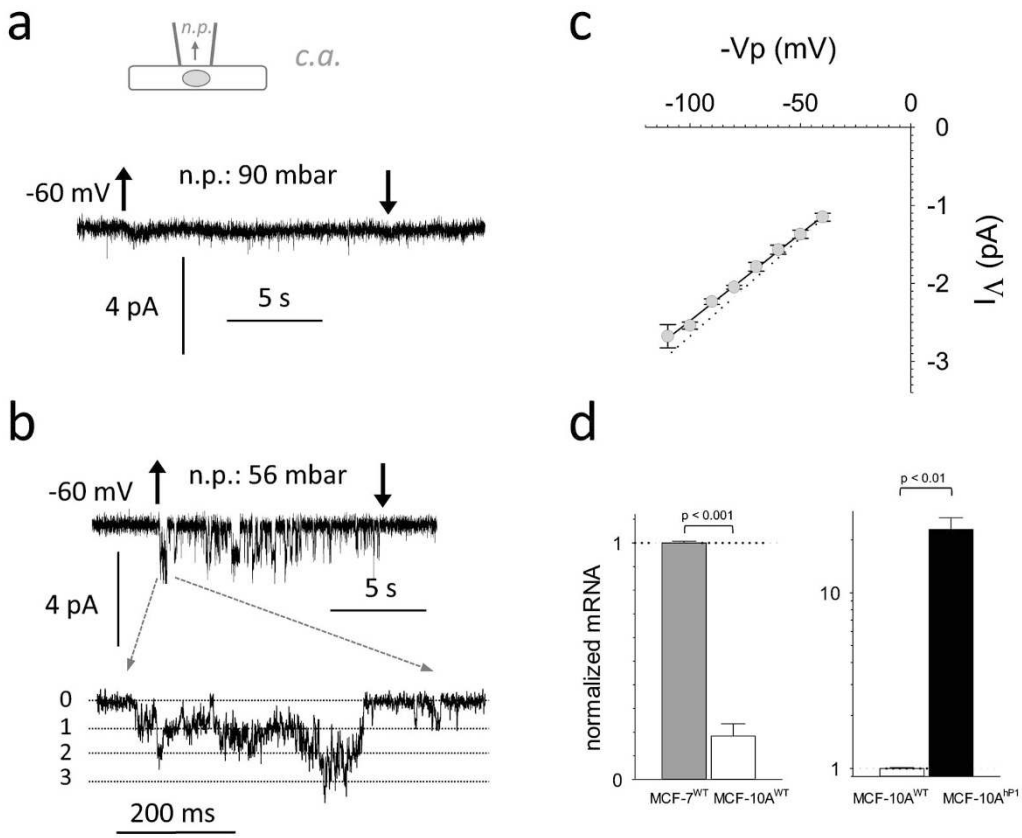

Figure 5 | Single channel conductance properties of hPiezo1 expressed in the MCF-10A cell line. (5a).: Original registration from untransfected MCF-10A cell (configuration shown schematically at top). (5b).: same as 5A, but cell was transfected with biscistronic pIRES2 containing hPiezo1 and eGFP as inserts. (5c).: Average I/V relation for single I_Λ inward currents carried by 153 mmole/L K^+. Line represents a linear regression through the data (N = 5), dotted line represents average I_Λ recorded from HEK-293 cells under identical conditions. (5d).: left: Quantitative RT-PCR assessing the relative amount of hPiezo1 mRNA transcripts of MCF-10A^{WT} cells compared to MCF-7^{WT}. Mean values ± SEM are shown (N = 3). Right: the fold increase in the number of hPiezo1 mRNA transcripts upon transient transfection of MCF-10A with the pIRES2 construct. Mean values ± SEM are shown (N = 3).

in MCF-7 cells: (i) G_Λ's were indistinguishable between MSCs from MCF-7 and MSCs formed by overexpressed Piezo1 in HEK-293 cells. (ii) The particular ion permeation properties with respect to G_Λ's for different ions as described above were identical between MSCs from MCF-7 and Piezo1 overexpressed in HEK-293 cells. (iii) MSCs in cell attached patches of MCF-7 cells exerted similar mechanical sensitivity when compared to MSCs formed by overexpression of Piezo1 in HEK-293[13,24] as well as in MCF-10A cells and (iv) MSCs in MCF-7 disclosed themselves to be completely unreactive to global knockout of MSCs formed by canonical Trp subunits.

When the benign MEC line MCF-10A was screened via the patch clamp method, no functional MSCs were observed. Expression levels for mRNA encoding Piezo1 were substantially lower when compared to MCF-7, but not negligible. In this context it is worth mentioning that the cDNA encoding human Piezo1 has been initially cloned from wild-type HEK-293 cells[24]. This cell line is, however, frequently used as a negative control, both in biochemical and electrophysiological experiments, demonstrating that its endogenous mRNA levels are not sufficient to produce high amount of Piezo1 protein[13]. Thus a low density (or even absence) of functional MSCs in the plasma membrane despite of moderate mRNA levels is not an unusual situation. Several scenarios may account for the absence of functional MSCs in native MCF-10A cells: (i) Endogenous mRNA encoding Piezo1 does not produce MSCs at sufficient high numbers to allow reliable detection by the patch clamp method. (ii) The resulting small amount of protein is not inserted into the plasma membrane. (iii) Endogenous Piezo1 protein is directed towards protein complexes, where it cannot be activated by simple mechanical stimulation and only heterologous Piezo1, inserted somewhere else, is accessible to this stimulation or (iv) endogenous Piezo1 is blocked by endogenous factors that become rate limiting upon overexpression (see e.g.: ref. 30).

Several studies have addressed the effects of mechanical stress on cancerogenesis and tumor progression in benign and malign MECs and thereupon may shed light on potential roles of increased densities of MSCs in the plasma membrane of malignant MECs : When the effect of compressive stress on proliferation, apoptosis, migration and cytoskeletal architecture of several MECs, including MCF-10A and MCF-7, was studied, malign breast carcinoma cell lines, but not MCF-10A responded to compressive stress with the development of a more aggressive phenotype. The authors of the study concluded that non-tumorigenic MCF-10A cells are less mechanosensitive as their malign counterparts[31]. Using a microlithography based approach it was found that proliferation and invasion of several lines of malignant MECs, embedded in non-malignant tissue, occurred preferentially in regions characterized by high endogenous mechanical stress; this observation substantiates the role of mechanical stress in promoting the malignant phenotype[32]. In another study the impact of long-range mechanical interaction exerted via collagen lines on the disorganization of ras-transformed mammary acini formed by MCF-10AT cells was investigated. Mechanical interaction between MCF-10AT acini was shown to facilitate the transition to the invasive phenotype whereas mechanical isolation of acini impaired it[33]. Taken together, the general role of mechanical stress in etiology and progression of breast cancer as well as the impact of mechanosignaling on growth, invasion and differentiation of pecu-

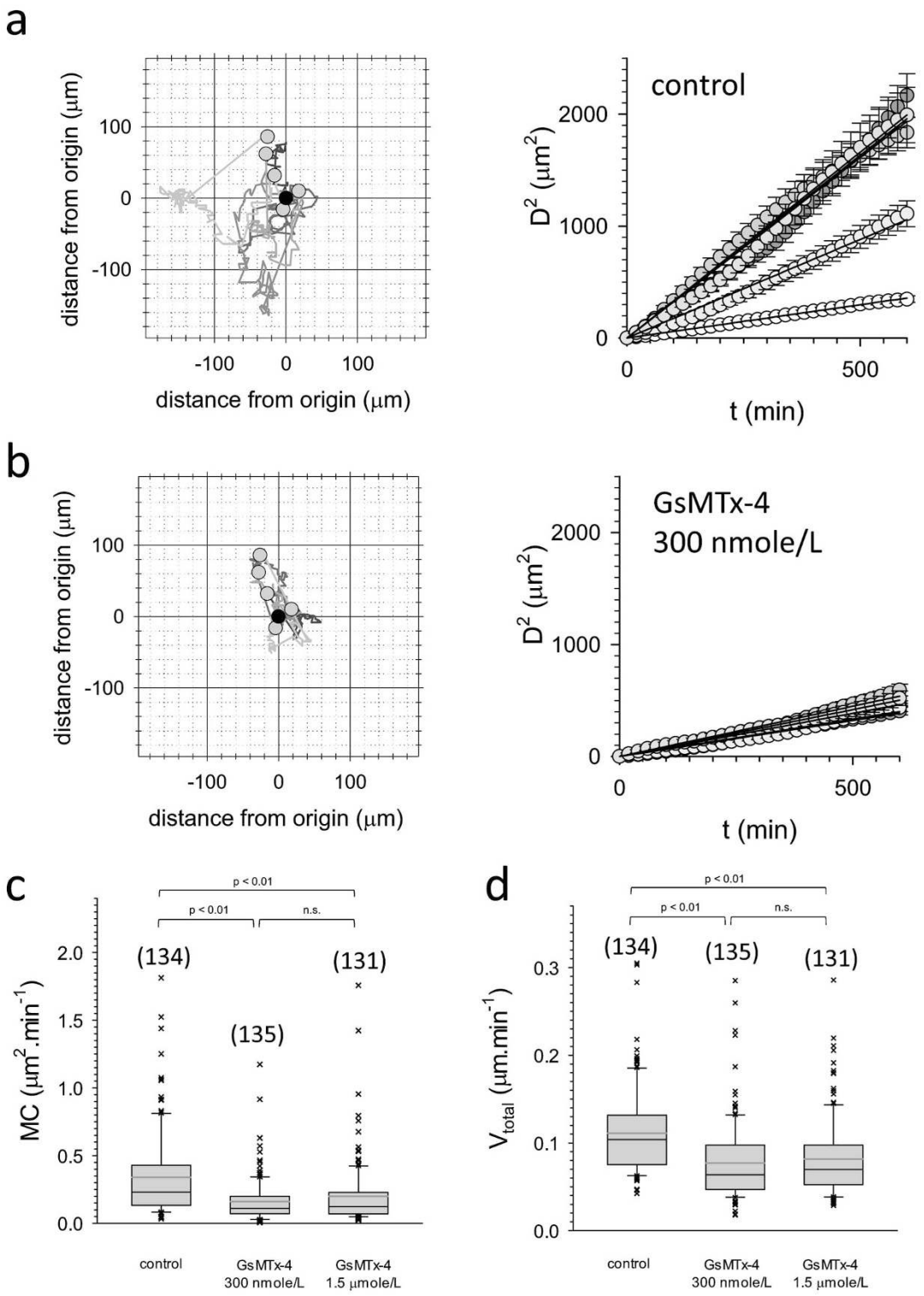

Figure 6 | Effect of GsMTx-4 on migration and velocity of MCF-7 cells. (6a).: left: Migration trajectories of five single MCF-7^{WT} cells over the entire observation interval of 72h. Right: Squared distance as a function of time for the five cells shown to the left. (6b).: similar to 6a but in the presence of 300 nmole/L GsMTx-4. (6c).: statistical analysis of motility coefficients. Black line in box marks median, upper and lower borders of box mark 25th and 75th percentiles, whiskers mark 10th and 90th percentiles, respectively; black crosses mark individual single cell velocities below and above the 10th and 90th percentiles. Grey line marks mean value. Number of individual cells studied is shown in parenthesis above each box. The dataset was checked for statistical significant differences using ANOVA based on ranks. (6d).: similar to 6c but cellular velocities are shown.

liar MECs is well studied[34]. The findings described above fit reasonable to the hypothesis that a high density of MSCs in malignant MECs intensifies their reaction to mechanical cues, thereby promoting malignancy. It must be stated, however, that mechanosensation by MECs is generally considered to be based on a molecular machinery that does not necessarily entail ion channels: The molecular chain of events comprises ligands of the extracellular matrix or from neighboring cells that bind to integrins thereby inducing integ-

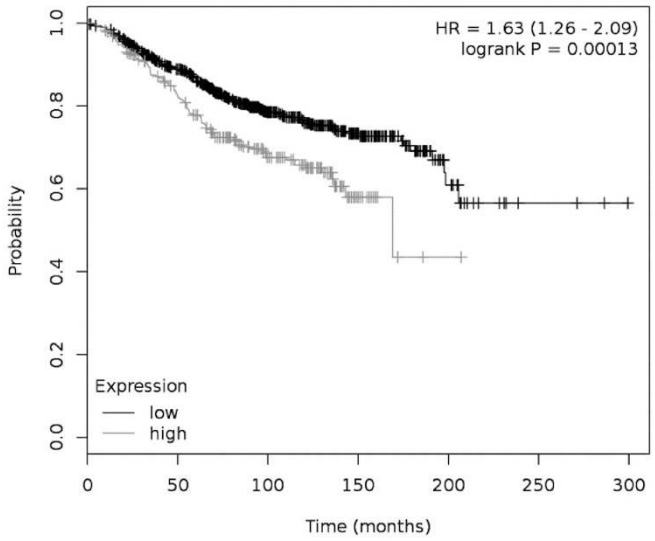

Figure 7 | Overall survival of breast cancer patients with low and high expression of Piezo1 mRNA in the primary tumor. Kaplan–Meier plot showing overall survival of breast cancer patients with low and high expression levels of Piezo1 mRNA. Grey line: patients with high expression of Piezo1; black line: patients with low expression (cutoff value was 1760 tpm (transcripts per million)). Hazard ratio (HR) was 1.63 (1.26–2.09; 95% confidence interval), $P < 0.000013$, $N = 1115$).

rin clustering, formation of focal adhesion sites and subsequent activation of focal adhesion kinase, a central intracellular effector of mechanotransduction[35]. Many different protein subunits (integrin-adhesome), but also elements of the glycocalyx, have been identified to participate in and to regulate this process[36,37]. Consequently we may ask whether MSCs formed by Piezo1 are hitherto unrecognized constituents of this molecular machinery. Few reports foster the view that Piezo1 represents an integral part of the former pathway since they demonstrate that Ca^{2+} entry through MSCs of the plasma membrane is required to trigger integrin-dependent mechanoreception[38,39]. In addition, it is notable that the first biological function found for Piezo1 protein was integrin activation by increasing intracellular Ca^{2+} levels: Expression of a Piezo1/GFP chimera (that was localized predominantly to the endoplasmic reticulum) in CHO cells, triggered integrin dependent cell adhesion while knockout of Piezo1 resulted in the opposite[40]. Thus it is possible that Piezo1 may be part of and a trigger for the integrin mechanosensation machinery. Upon overexpression of Piezo1 in malignant MCF-7 cells this machinery becomes hyperactive. On the other hand Piezo1 ion channels may also provide a separate and parallel pathophysiological mechanosignal transduction pathway providing malign MECs with a sensorium for mechanical cues that acts in addition to integrin signaling. More experimentation is required to allocate the exact location of Piezo1 in the molecular landscape of MEC mechanotransduction. Which mechanism is operative in MCF-7 cells is currently under investigation.

Albeit the Fam38A and Fam38B gene products (i.e.: Piezo1 and Piezo2) have been identified only recently as templates for mechanosensitive ion channel proteins[13], several physiological functions have been identified so far: While Piezo2 protein is involved in somatosensation of touch[41], several roles for Piezo1 protein outside the nervous system have been found. Piezo1 plays a role in live cell extrusion, a phenomenon that is important to maintain homeostatic cell numbers in epithelia[42], senses shear stress in vascular endothelial cells, being important for embryonic development of the circulatory system[43,44] and triggers the response of urothelium to bladder extension[45]. Gain of function mutations in both Piezo1 and Piezo2 protein have been identified as the basis for different pathologies such as xerocytosis and distal arthrogryposis[24,46]. In addition to our findings other data suggest that Piezo1 protein is also involved in cancer: Most intense expression of mRNAs encoding Piezo1, amongst the tissues studied, has been found in the lung and also in lung epithelial cells, where its physiological role still remains to be shown[13,47]. Loss of Piezo1 in normal lung epithelial cells promoted an amoeboid, reduced integrin-dependent, mode of cell migration, that is a typical phenotype of small lung cancer cells where Piezo1 expression was found to be greatly reduced[47]. In the prevailing study we observed the opposite, i.e. that mRNA expression was low in benign MECs, but higher expression levels led to functional MSCs within the plasma membrane of the malign MCF-7 cell line, affecting cell migration. Similar to our results, knockdown of Piezo1 in gastric epithelium cancer cells has been shown to reduce cell migration and the authors suggested that Piezo1 overexpression promotes invasion and metastasation of gastric cancer[48]. Piezo1 was also amongst the most profoundly upregulated genes in thyroid cancers following Iodine-131 exposure after the Chernobyl accident[49], indicating that deregulated Piezo1 expression may contribute to cancer of several tissue types. The role of Piezo1 in progression of breast cancer is substantiated by the significantly increased hazard ratio and corresponding shorter overall survival times of breast cancer patients upon high mRNA expression levels in the primary tumor reported here. This novel role of Piezo1 in cancer biology seems to be a peculiar manifestation in breast cancer that is different to the role of Piezo1 in lung cancer. Further research will reveal whether Piezo1 is causally involved in cancerogenesis and progression of breast cancer, represents a potential therapeutic target or can be used as a prognostic factor.

1. Shieh, A. C. Biomechanical forces shape the tumor microenvironment. *Annals of biomedical engineering* **39**, 1379–1389, doi:10.1007/s10439-011-0252-2 (2011).
2. Bukoreshtliev, N. V., Haase, K. & Pelling, A. E. Mechanical cues in cellular signalling and communication. *Cell and Tissue Research* **352**, 77–94, doi:10.1007/s00441-012-1531-4 (2013).
3. Mammoto, T. & Ingber, D. E. Mechanical control of tissue and organ development. *Development* **137**, 1407–1420, doi:10.1242/dev.024166 (2010).
4. Butcher, D. T., Alliston, T. & Weaver, V. M. A tense situation: forcing tumour progression. *Nat Rev Cancer* **9**, 108–122 (2009).
5. Schedin, P. & Keely, P. J. Mammary gland ECM remodeling, stiffness, and mechanosignaling in normal development and tumor progression. *Cold Spring Harbor perspectives in biology* **3**, a003228, doi:10.1101/cshperspect.a003228 (2011).
6. Nelson, C. M. & Bissell, M. J. Of extracellular matrix, scaffolds, and signaling: tissue architecture regulates development, homeostasis, and cancer. *Annual review of cell and developmental biology* **22**, 287–309, doi:10.1146/annurev.cellbio.22.010305.104315 (2006).
7. Michor, F., Liphardt, J., Ferrari, M. & Widom, J. What does physics have to do with cancer? *Nat Rev Cancer* **11**, 657–670, doi:10.1038/nrc3092 (2011).
8. Yu, H. M., Mouw, J. K. & Weaver, V. M. Forcing form and function: biomechanical regulation of tumor evolution. *Trends in Cell Biology* **21**, 47–56, doi:10.1016/j.tcb.2010.08.015 (2011).
9. Geiger, B., Spatz, J. P. & Bershadsky, A. D. Environmental sensing through focal adhesions. *Nature reviews. Molecular cell biology* **10**, 21–33, doi:10.1038/nrm2593 (2009).
10. Sukharev, S. & Sachs, F. Molecular force transduction by ion channels: diversity and unifying principles. *J Cell Sci* **125**, 3075–3083, doi:10.1242/jcs.092353 (2012).
11. Wu, L. J., Sweet, T. B. & Clapham, D. E. International Union of Basic and Clinical Pharmacology. LXXVI. Current progress in the mammalian TRP ion channel family. *Pharmacological reviews* **62**, 381–404, doi:10.1124/pr.110.002725 (2010).
12. Patel, A. *et al.* Canonical TRP channels and mechanotransduction: from physiology to disease states. *Pflugers Archiv : European journal of physiology* **460**, 571–581, doi:10.1007/s00424-010-0847-8 (2010).
13. Coste, B. *et al.* Piezo proteins are pore-forming subunits of mechanically activated channels. *Nature* **483**, 176–181, doi:10.1038/nature10812 (2012).
14. Kawashima, Y., Kurima, K., Pan, B., Griffith, A. J. & Holt, J. R. Transmembrane channel-like (TMC) genes are required for auditory and vestibular mechanosensation. *Pflugers Archiv : European journal of physiology*, doi:10.1007/s00424-014-1582-3 (2014).
15. Prevarskaya, N., Skryma, R. & Shuba, Y. Ion channels and the hallmarks of cancer. *Trends in Molecular Medicine* **16**, 107–121, doi:10.1016/j.molmed.2010.01.005 (2010).
16. Lee, J., Ishihara, A., Oxford, G., Johnson, B. & Jacobson, K. Regulation of cell movement is mediated by stretch-activated calcium channels. *Nature* **400**, 382–386, doi:10.1038/22578 (1999).

17. Wagner, V. *et al.* Cloning and characterisation of GIRK1 variants resulting from alternative RNA editing of the KCNJ3 gene transcript in a human breast cancer cell line. *Journal of cellular biochemistry* **110**, 598–608, doi:10.1002/jcb.22564 (2010).
18. Scheruebel, S. *et al.* I(f) blocking potency of ivabradine is preserved under elevated endotoxin levels in human atrial myocytes. *J Mol Cell Cardiol* **72**, 64–73, doi:10.1016/j.yjmcc.2014.02.010 (2014).
19. Livak, K. J. & Schmittgen, T. D. Analysis of Relative Gene Expression Data Using Real-Time Quantitative PCR and the 2−ΔΔCT Method. *Methods* **25**, 402–408, doi:http://dx.doi.org/10.1006/meth.2001.1262 (2001).
20. Poteser, M. *et al.* PKC-dependent coupling of calcium permeation through transient receptor potential canonical 3 (TRPC3) to calcineurin signaling in HL-1 myocytes. *Proc Natl Acad Sci U S A* **108**, 10556–10561, doi:10.1073/pnas.1106183108 (2011).
21. Maroto, R. *et al.* TRPC1 forms the stretch-activated cation channel in vertebrate cells. *Nature cell biology* **7**, 179–185, doi:10.1038/ncb1218 (2005).
22. Cahalan, M. D. & Parker, I. Choreography of cell motility and interaction dynamics imaged by two-photon microscopy in lymphoid organs. *Annu Rev Immunol* **26**, 585–626, doi:10.1146/annurev.immunol.24.021605.090620 (2008).
23. Gyorffy, B. *et al.* An online survival analysis tool to rapidly assess the effect of 22,277 genes on breast cancer prognosis using microarray data of 1,809 patients. *Breast Cancer Res Treat* **123**, 725–731, doi:10.1007/s10549-009-0674-9 (2010).
24. Bae, C., Gnanasambandam, R., Nicolai, C., Sachs, F. & Gottlieb, P. A. Xerocytosis is caused by mutations that alter the kinetics of the mechanosensitive channel PIEZO1. *Proc Natl Acad Sci U S A* **110**, E1162–1168, doi:10.1073/pnas.1219777110 (2013).
25. Gottlieb, P. A., Bae, C. & Sachs, F. Gating the mechanical channel Piezo1: a comparison between whole-cell and patch recording. *Channels* **6**, 282–289, doi:10.4161/chan.21064 (2012).
26. Neve, R. M. *et al.* A collection of breast cancer cell lines for the study of functionally distinct cancer subtypes. *Cancer Cell* **10**, 515–527, doi:10.1016/j.ccr.2006.10.008 (2006).
27. Soule, H. D. *et al.* Isolation and characterization of a spontaneously immortalized human breast epithelial cell line, MCF-10. *Cancer Res* **50**, 6075–6086 (1990).
28. Hanahan, D. & Weinberg, R. A. Hallmarks of cancer: the next generation. *Cell* **144**, 646–674, doi:10.1016/j.cell.2011.02.013 (2011).
29. Bae, C., Sachs, F. & Gottlieb, P. A. The Mechanosensitive Ion Channel Piezo1 Is Inhibited by the Peptide GsMTx4. *Biochemistry* **50**, 6295–6300, doi:10.1021/bi200770q (2011).
30. Peyronnet, R. *et al.* Piezo1-dependent stretch-activated channels are inhibited by Polycystin-2 in renal tubular epithelial cells. *Embo Reports* **14**, 1143–1148, doi:10.1038/embor.2013.170 (2013).
31. Tse, J. M. *et al.* Mechanical compression drives cancer cells toward invasive phenotype. *Proceedings of the National Academy of Sciences of the United States of America* **109**, 911–916, doi:10.1073/pnas.1118910109 (2012).
32. Boghaert, E. *et al.* Host epithelial geometry regulates breast cancer cell invasiveness. *Proceedings of the National Academy of Sciences of the United States of America* **109**, 19632–19637, doi:10.1073/pnas.1118872109 (2012).
33. Shi, Q. *et al.* Rapid disorganization of mechanically interacting systems of mammary acini. *Proc Natl Acad Sci U S A* **111**, 658–663, doi:10.1073/pnas.1311312110 (2014).
34. DuFort, C. C., Paszek, M. J. & Weaver, V. M. Balancing forces: architectural control of mechanotransduction. *Nature reviews. Molecular cell biology* **12**, 308–319, doi:10.1038/nrm3112 (2011).
35. Provenzano, P. P., Inman, D. R., Eliceiri, K. W. & Keely, P. J. Matrix density-induced mechanoregulation of breast cell phenotype, signaling and gene expression through a FAK-ERK linkage. *Oncogene* **28**, 4326–4343, doi:10.1038/onc.2009.299 (2009).
36. Zaidel-Bar, R., Itzkovitz, S., Ma'ayan, A., Iyengar, R. & Geiger, B. Functional atlas of the integrin adhesome. *Nat Cell Biol* **9**, 858–867, doi:10.1038/ncb0807-858 (2007).
37. Paszek, M. J. *et al.* The cancer glycocalyx mechanically primes integrin-mediated growth and survival. *Nature* **511**, 319–325, doi:10.1038/nature13535 (2014).
38. Ross, T. D. *et al.* Integrins in mechanotransduction. *Current opinion in cell biology* **25**, 613–618, doi:10.1016/j.ceb.2013.05.006 (2013).
39. Martinac, B. The ion channels to cytoskeleton connection as potential mechanism of mechanosensitivity. *Biochimica et biophysica acta* **1838**, 682–691, doi:10.1016/j.bbamem.2013.07.015 (2014).
40. McHugh, B. J. *et al.* Integrin activation by Fam38A uses a novel mechanism of R-Ras targeting to the endoplasmic reticulum. *J Cell Sci* **123**, 51–61, doi:10.1242/jcs.056424 (2010).
41. Woo, S. H. *et al.* Piezo2 is required for Merkel-cell mechanotransduction. *Nature* **509**, 622–626, doi:10.1038/nature13251 (2014).
42. Eisenhoffer, G. T. *et al.* Crowding induces live cell extrusion to maintain homeostatic cell numbers in epithelia. *Nature* **484**, 546–549, doi:10.1038/nature10999 (2012).
43. Ranade, S. S. *et al.* Piezo1, a mechanically activated ion channel, is required for vascular development in mice. *Proc Natl Acad Sci U S A* **111**, 10347–10352, doi:10.1073/pnas.1409233111 (2014).
44. Li, J. *et al.* Piezo1 integration of vascular architecture with physiological force. *Nature*, doi:10.1038/nature13701 (2014).
45. Miyamoto, T. *et al.* Functional Role for Piezo1 in Stretch-evoked Ca2+ Influx and ATP Release in Urothelial Cell Cultures. *The Journal of biological chemistry* **289**, 16565–16575, doi:10.1074/jbc.M113.528638 (2014).
46. Coste, B. *et al.* Gain-of-function mutations in the mechanically activated ion channel PIEZO2 cause a subtype of Distal Arthrogryposis. *Proc Natl Acad Sci U S A* **110**, 4667–4672, doi:10.1073/pnas.1221400110 (2013).
47. McHugh, B. J., Murdoch, A., Haslett, C. & Sethi, T. Loss of the integrin-activating transmembrane protein Fam38A (Piezo1) promotes a switch to a reduced integrin-dependent mode of cell migration. *PloS one* **7**, e40346, doi:10.1371/journal.pone.0040346 (2012).
48. Yang, X. N. *et al.* Piezo1 is as a novel trefoil factor family 1 binding protein that promotes gastric cancer cell mobility in vitro. *Dig Dis Sci* **59**, 1428–1435, doi:10.1007/s10620-014-3044-3 (2014).
49. Abend, M. *et al.* Iodine-131 dose dependent gene expression in thyroid cancers and corresponding normal tissues following the Chernobyl accident. *PloS one* **7**, e39103, doi:10.1371/journal.pone.0039103 (2012).

Acknowledgments

M. Absenger (Core Facility Microscopy/ZMF, MUG, Graz, Austria) provided technical assistance for using the cell observer. We thank A. Patapoutian (HHMI, La Jolla, CA, USA) for providing the plasmid (pIRES2) containing the human Piezo1 and eGFP cDNA. Financial support by the Austrian Research Foundation is gratefully acknowledged (FWF P22974-B19 (W.S.); KLIF 182 (T.B.); W1226-B18 (E.M.)).

Author contributions

C.L. and W.S. performed patch clamp experiments. S.R., S.K., A.G. and S.J. performed molecular biology experiments. C.L., S.R., A.S., T.dV. and W.S. performed experiments with and analyzed data from the cell observer. S.K., A.S., H.H., C.W. and W.S. performed data mining and biostatistics. C.L., A.S. and W.S. prepared the figures. C.L. and W.S. wrote the main manuscript text. C.L., S.R., S.K., A.S., T.dV., A.G., S.J., H.H., K.G., C.W., E.M., T.B. and W.S. participated in discussions on and planning of experiments. All authors reviewed the manuscript.

Additional information

Supplementary information accompanies this paper at http://www.nature.com/scientificreports

Competing financial interests: The authors declare no competing financial interests.

How to cite this article: Li, C. *et al.* Piezo1 forms mechanosensitive ion channels in the human MCF-7 breast cancer cell line. *Sci. Rep.* **5**, 8364; DOI:10.1038/srep08364 (2015).